ARMY RESEARCH LABORATORY

Computational Modeling of a Segmented Projectile

Jubaraj Sahu
Karen R. Heavey

ARL-TR-1988 JUNE 1999

The findings in this report are not to be construed as an official Department of the Army position unless so designated by other authorized documents.

Citation of manufacturer's or trade names does not constitute an official endorsement or approval of the use thereof.

Destroy this report when it is no longer needed. Do not return it to the originator.

Army Research Laboratory
Aberdeen Proving Ground, MD 21005-5066

ARL-TR-1988 June 1999

Computational Modeling of a Segmented Projectile

Jubaraj Sahu
Karen R. Heavey
Weapons & Materials Research Directorate, ARL

Abstract

This report describes the application of the chimera numerical technique to a multi-body segmented projectile configuration system of interest to the U.S. Army. Computations were performed at a supersonic speed on this configuration which consists of an ogive-cylinder projectile with a peg-shaped trailing segment. The computed results show the qualitative features of the wake flow field for the projectile with the segment in three different positions: centered, offset, and angled. The segment in the offset position has a strong effect on the flow field in the aft region of the projectile, thus affecting the aerodyamic coeffiecients of the projectile. The force and moment coefficients of the segment are also significantly affected by the orientation of the segment.

ACKNOWLEDGMENTS

The authors wish to thank Dr. Edward Schmidt, U.S. Army Research Laboratory Senior Research Scientist (Ballistics Research) for his interest and support of this work. His technical expertise was a great help in the research effort undertaken to model the aerodynamic behavior of this multi-body projectile system.

INTENTIONALLY LEFT BLANK

TABLE OF CONTENTS

INTENTIONALLY LEFT BLANK

LIST OF FIGURES

INTENTIONALLY LEFT BLANK

LIST OF TABLES

INTENTIONALLY LEFT BLANK

COMPUTATIONAL MODELING OF A SEGMENTED PROJECTILE

1. INTRODUCTION

Aerodynamic forces and moments are critical design parameters used in the design of artillery shells and bodies flying in relative motion to each other. The advancement of computational fluid dynamics (CFD) is beginning to have a major impact on projectile design and development.**[1-4]** Improved computer technology and state-of-the-art numerical procedures enable scientists to develop solutions to complex, three-dimensional (3-D) problems associated with projectile and missile aerodynamics. The research effort has focused on the development and application of a versatile overset grid numerical technique to solve geometrically complex single-body as well as multi-body aerodynamic problems. This numerical capability has been used successfully to determine the aerodynamics on a number of multi-body projectile configurations **[4-6]** at transonic and supersonic speeds. Earlier applications involved axisymmetric flow computations.**[4,5]** Recently, this technique has been used to investigate the submunition dispersal from an Army tactical missile system **[6]** involving 3-D flow computations. This report describes the application of the advanced numerical technique to a multi-body segmented projectile configuration of interest to the U.S. Army. Figure 1 shows a computational model for this system, with several trailing segments centered along the line of symmetry in the wake of the projectile. This multi-body problem involves 3-D flow computations of trailing segments flying in the wake of a parent projectile. However, the scope of this study is limited to one trailing segment. The particular problem here is to determine the resulting aerodynamic interference with the segment in centered, offset, and angled positions.

Figure 1. Computational Model for a Segmented Projectile.

The complexity and uniqueness of this type of multi-body problem result from the aerodynamic interference of the individual components, which include 3-D shock-shock interactions, shock-boundary layer interactions, and highly viscous-dominated separated wake flow regions. The overset grid technique **[7-9]**, which is ideally suited to this problem, involves generating numerical grids about each body component and then oversetting them onto a base grid

to form the complete model. With this composite overset grid approach, it is possible to determine the 3-D interacting flow field of the multi-body system and the associated aerodynamic forces and moments at different positions and orientations without the need for costly regridding. The solution procedure of the developed technique is to compute the interference flow field at multiple locations until final converged solutions are obtained and then to integrate the pressure and viscous forces to obtain the total forces and moments.

A description of the computational algorithm and the chimera technique follows. The next section describes the model geometry and various computational grids used in the numerical computations. Steady state computational results are presented for various orientations and locations of the segment in the projectile's wake.

2. SOLUTION TECHNIQUE

The complete set of time-dependent, Reynolds-averaged, thin layer Navier-Stokes equations is solved numerically to obtain a solution to this problem. The numerical technique used is an implicit, finite difference scheme. Time-accurate calculations are made to numerically simulate the submunition in three possible positions relative to the main projectile.

2.1 Governing Equations

The complete set of 3-D, time-dependent, generalized geometry, Reynolds-averaged, thin layer Navier-Stokes equations for general spatial coordinates ξ, η, and ζ can be written as follows **[10]**:

$$\partial_\tau \hat{q} + \partial_\xi \hat{F} + \partial_\eta \hat{G} + \partial_\zeta \hat{H} = Re^{-1} \partial_\zeta \hat{S}, \qquad (1)$$

where

$\xi = \xi(x, y, z, t)$ - longitudinal coordinate;
$\eta = \eta(x, y, z, t)$ - circumferential coordinate;
$\zeta = \zeta(x, y, z, t)$ - nearly normal coordinate;
$\tau = t$ - time

In Equation 1, $\hat{q}$ contains the dependent variables: density, three velocity components, and energy. The thin layer approximation is used here, and the viscous terms involving velocity gradients in both the longitudinal and circumferential directions are neglected. The viscous terms are retained in the normal direction, ζ, and are collected into the vector $\hat{S}$. These viscous terms are used everywhere. In the wake or the base region, similar viscous terms are also added in the streamwise direction, ξ. An implicit, approximately factored scheme is used to solve these equations.

2.2 Numerical Algorithm

The implicit, approximately factored scheme for the thin layer Navier-Stokes equations using central differencing in the η and ζ directions and "upwinding" in ξ is written in the following form **[11]**:

$$\begin{aligned}
&\left[I + i_b h \delta_\xi^b \left(\hat{A}^+ \right)^n + i_b h \delta_\zeta \hat{C}^n - i_b h \, Re^{-1} \overline{\delta}_\zeta J^{-1} \hat{M}^n J - i_b D_i |_\zeta \right] \\
&\quad \times \left[I + i_b h \delta_\xi^f \left(\hat{A}^- \right)^n + i_b h \delta_\eta \hat{B}^n - i_b D_i |_\eta \right] \Delta \hat{Q}^n \\
&= i_b \Delta t \left\{ \delta_\xi^b \left[\left(\hat{F}^+ \right)^n - \hat{F}_\infty^+ \right] + \delta_\xi^f \left[\left(\hat{F}^- \right)^n - \hat{F}_\infty^- \right] + \delta_\eta \left(\hat{G}^n - \hat{G}_\infty \right) \right. \\
&\quad \left. + \delta_\zeta \left(\hat{H}^n - \hat{H}_\infty \right) - Re^{-1} \overline{\delta}_\zeta \left(\hat{S}^n - \hat{S}_\infty \right) \right\} - i_b D_e \left(\hat{Q}^n - \hat{Q}_\infty \right),
\end{aligned} \tag{2}$$

where h = Δt and the free-stream base solution is used. Here, δ is typically a three-point second order accurate central difference operator, $\overline{\delta}$ is a midpoint operator used with the viscous terms, and the operators δ_ξ^b and δ_ξ^f are backward and forward three-point difference operators. The flux $\hat{F}$ has been eigensplit, and the matrices $\hat{A}, \hat{B}, \hat{C}$, and $\hat{M}$ result from local linearization of the fluxes about the previous time level. Here, J denotes the Jacobian of the coordinate transformation. Dissipation operators D_e and D_i are used in the central space differencing directions. The smoothing terms used in the present study are of the form

$$D_e|_\eta = (\Delta t) J^{-1} \left[\varepsilon_2 \overline{\delta} \rho(B) \beta \overline{\delta} + \varepsilon_4 \overline{\delta} \, \frac{\rho(B)}{1+\beta} \overline{\delta}^3 \right] |_\eta \, J,$$

and

$$D_i|_\eta = (\Delta t) J^{-1} \left[\varepsilon_2 \overline{\delta} \rho(B) \beta \overline{\delta} + 2.5 \varepsilon_4 \overline{\delta} \rho(B) \overline{\delta} \right] |_\eta \, J,$$

where

$$\beta = \frac{\left| \overline{\delta}^2 P \right|}{\left| \left(1 + \delta^2 \right) P \right|},$$

and $\rho(B)$ is the true spectral radius of B. The idea here is that the fourth difference will be tuned down near shocks (e.g., as β gets large, the weight on the fourth difference drops down while the second difference tunes up).

2.3 Chimera Composite Grid Scheme

The chimera overset grid scheme **[7-9]** is a domain decomposition approach in which a configuration is meshed by using a collection of overset grids. It allows each component of the configuration to be gridded separately and overset into a main grid. Overset grids are not required to join in any special way. Usually, a major grid covers the entire domain or a grid is generated about a dominant body. Minor grids are generated about the rest of the other bodies. Because each component grid is generated independently, portions of one grid may lie within the solid boundary contained within another grid. Such points lie outside the computational domain and are excluded from the solution process.

In the segmented projectile study, the grids around the projectile body comprise the major grid, while the grid around the segment is the minor grid. The minor grid is completely overlapped by the major grid; thus, its outer boundary can obtain information by interpolation from the major grid. Similar data transfer or communication is needed from the minor grid to the major grid. However, a natural outer boundary that overlaps the two grids does not exist. The chimera technique creates an artificial boundary (also known as a hole boundary) between grids, which provides the required path for information transfer from the segment to the projectile grid. The resulting hole region is excluded from the flow-field solution in the projectile grid. Equation 2 has been modified for chimera overset grids by the introduction of the flag i_b to achieve just that. This i_b array accommodates the possibility of having arbitrary holes in the grid. The i_b array is defined so that $i_b = 1$ at normal grid points and $i_b = 0$ at hole points. Thus, when $i_b = 1$, Equation 2 becomes the standard scheme. When $i_b = 0$, however, the algorithm reduces to $\Delta\hat{Q}^n = 0$ or $\hat{Q}^{n+1} = \hat{Q}^n$, leaving $\hat{Q}$ unchanged at hole points. The set of grid points that forms the border between the hole points and the normal field points are called inter-grid boundary points. These points are updated by interpolating the solution from the overset grid that created the hole. Values of the i_b array and the interpolation coefficients needed for this update are provided by a separate algorithm.**[7]**

A major part of the chimera overset grid approach is the information transfer from one grid into another by means of the inter-grid boundary points. Again, this set of points defines the hole boundaries and outer boundaries of the minor grids. These points depend on the solutions in the overlapping regions. In the present work, the PEGSUS code **[12]** has been used to establish the linkages between the various grids that are required by the flow solver or aerodynamics code described earlier. These include the determination of the interpolation coefficients and the establishing chimera logic for bodies making holes in overlapping grids.

2.4 Boundary Conditions

For simplicity, most of the boundary conditions have been imposed explicitly.[1] An isothermal wall boundary condition is used on the body surface, and the no-slip boundary condition is used at the wall. The pressure at the wall is calculated by solving a combined momentum equation. Free-stream boundary conditions are used at the inflow boundary as well as at the outer boundary. A symmetry boundary condition is imposed at the circumferential edges of the grid, while a simple extrapolation is used at the down-stream boundary. A combination of symmetry and extrapolation boundary conditions is used at the center line (axis). For cases where the free-stream flow is supersonic, a nonreflection boundary condition is used at the outer boundary. A no-slip wall boundary condition is used on the body surface of the trailing segment. Boundary condition is not applied at the outer boundary of the trailing segment; instead, it is updated through the chimera interpolation procedure.

3. MODEL GEOMETRY AND COMPUTATIONAL GRID

The projectile model consists of an ogive-cylinder, 6 calibers long, with a peg-shaped trailing segment. The segment is 1.5 calibers long and is located 1 caliber behind the projectile. Figure 2 shows a cross-sectional view of the computational grid for the multi-body configuration. The entire grid system consists of approximately 2 million grid points and is split into five sections: a small grid in front of the projectile body, two grid zones along the projectile body, a large grid in the wake region of the projectile, and finally, a grid around the trailing segment. Each grid section was obtained separately and then combined/overset to provide the full grid. The total number of points in the longitudinal, circumferential, and radial directions for the projectile grids is 156x75x70. The projectile wake or the base region grid is 94x75x129 and the segment grid is 111x75x25. The projectile grids extend 2 calibers in the normal direction from the line of symmetry, while the segment grid extends only 0.1 caliber from the segment surface and is entirely embedded in the base region grid. A body-conforming grid was obtained for the segment and then overset to form the composite mesh shown in Figure 2. This case corresponds to the centered position, where the segment is centered on the line of symmetry, behind the projectile. The major grid corresponds to the grids for the projectile, including the wake, which are easily generated independently of the minor grid (grid for the segment). In this and all subsequent figures, a portion of the segment surface has been cut away, allowing a view of grid and/or flow field in the cavity.

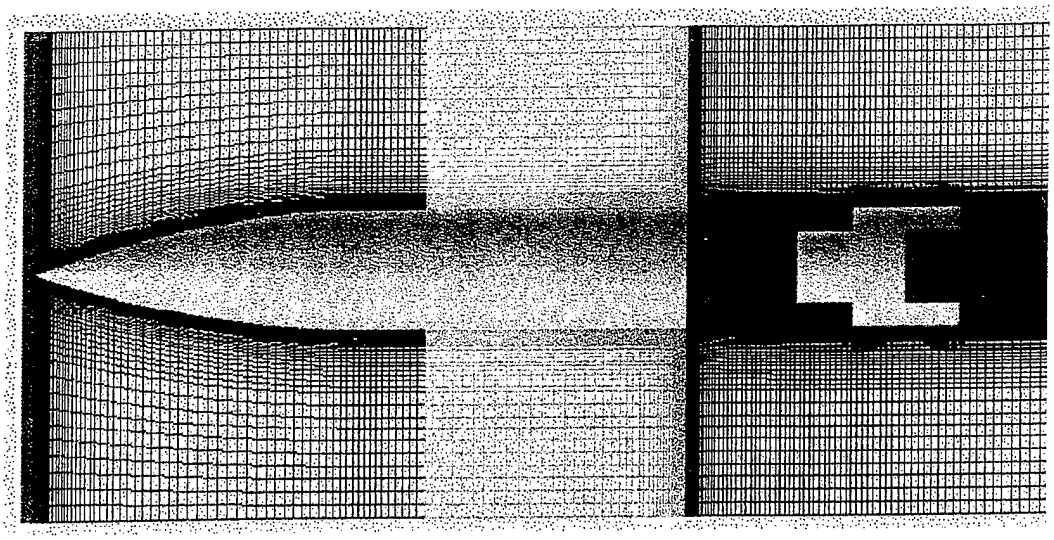

Figure 2. Computational Grid System.

As stated earlier, the chimera technique allows individual grids to be generated with any grid topology, thus making the grid generation process easier. For this study, the segment was initially positioned in the wake of the projectile, centered along the longitudinal line of symmetry. A geometric transformation was used to place it in both an offset and an angled position for additional configurations. Figure 3 shows an expanded view of the grid for each segment, embedded in the projectile wake. Again, there was no need to re-grid to generate the minor grid; a geometric transformation was used to place the original (centered) grid in the desired position. As part of the chimera blanking procedure, the segment cuts a hole in the base region grid of the projectile (see Figure 4). All grid points in the base region grid that lie within this hole are blanked and are excluded from the flow field solution process. Also, all points on this hole boundary in the base region grid are updated through interpolation of the solution in the segment grid. The grid blanking (hole cutting) shown in Figure 4 corresponds to the segment in the centered position. Similar hole cutting is done for other positions of the segment in the wake of the parent projectile.

4. RESULTS

In this study, 3-D steady state numerical computations were performed for the projectile alone and with a trailing segment in the three positions of interest described earlier. All computations were run at $M_\infty = 2.5$ and $\alpha = 0^\circ$, and atmospheric flight conditions were used. The calculations involving the trailing segment required approximately 45 million words of memory, and each case used an average of 30 hours of computer time on the Cray C-90 supercomputer at the Aeronautical Systems Center major shared resource center (MSRC). The

calculation for the projectile by itself used fewer resources and was done at the U.S. Army Research Laboratory MSRC on a Silicon Graphics platform.

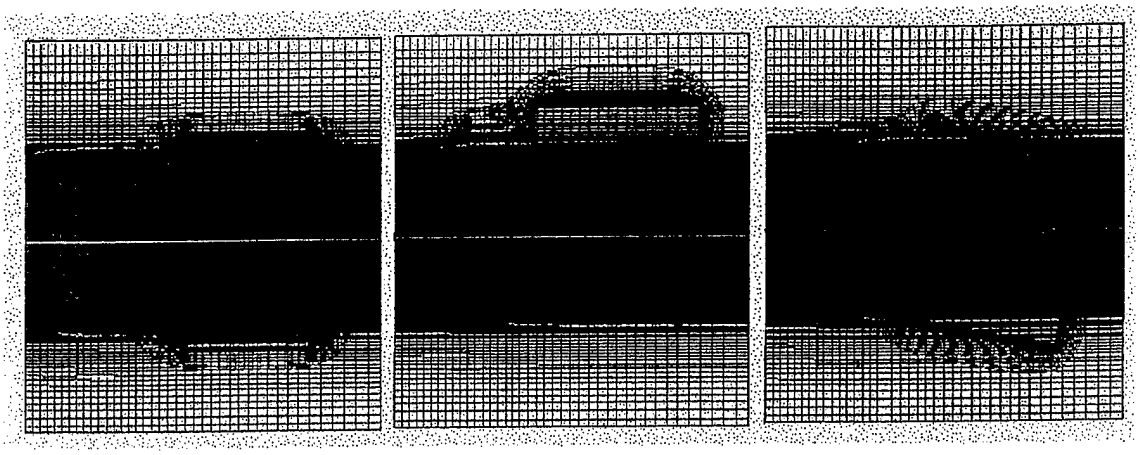

Figure 3. Grids for Segment in Three Positions: Centered, Offset, and Angled (left to right).

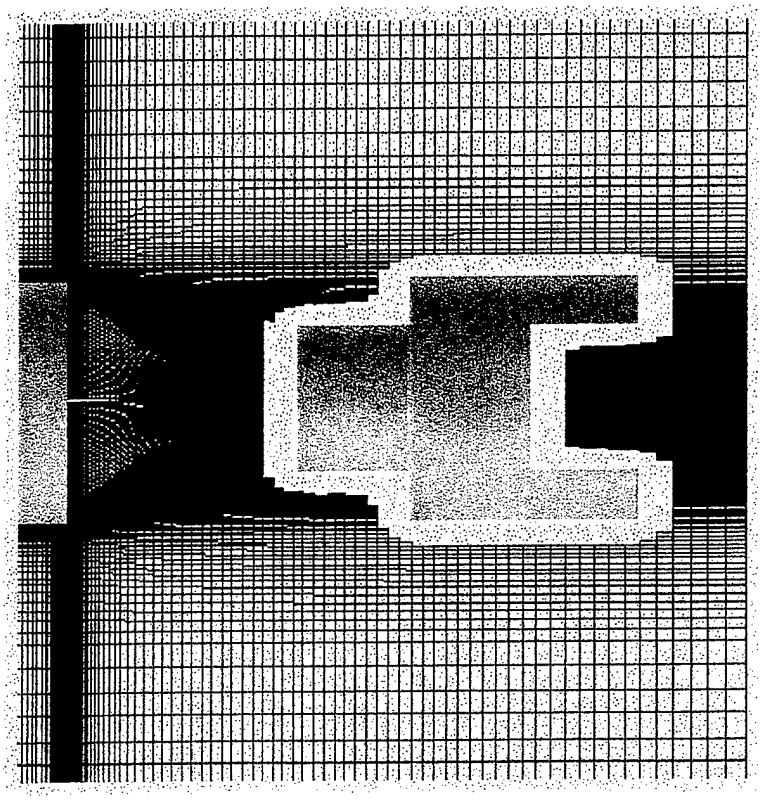

Figure 4. Background Grid Showing Chimera Blanking.

Results are shown first for the case when there is no trailing segment. Figures 5 and 6 show Mach contours and pressure contours, respectively. Here, blue represents low values and red represents high values of Mach and pressure contours. These figures clearly show the expected flow features. Figure 5 shows an oblique shock wave emanating from the nose of the projectile. The flow expands at the base corner, which is followed by a recompression shock down stream from the base. Figure 6 shows high pressures in the nose region and low pressures near the base. As expected, the flow field is quite symmetrical.

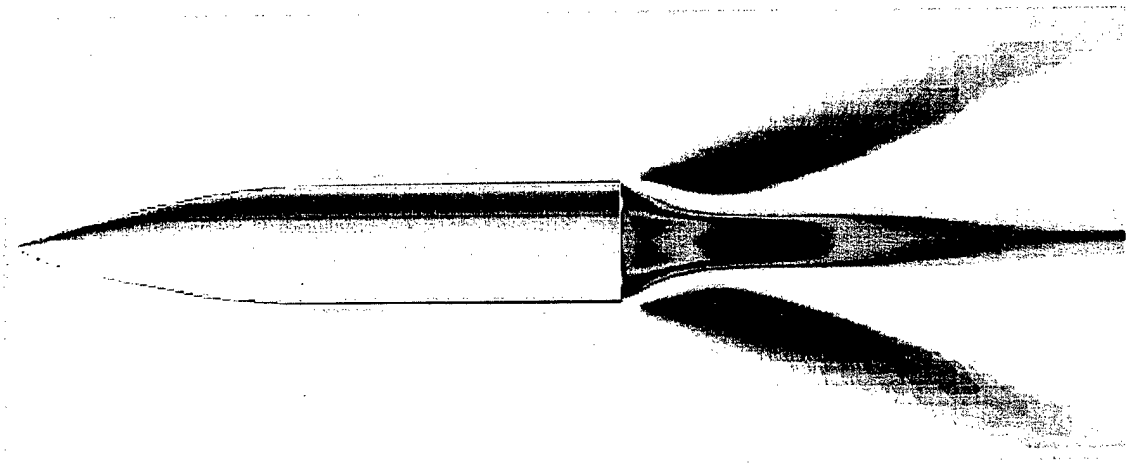

Figure 5. Mach Contours for a Projectile Without Segments.

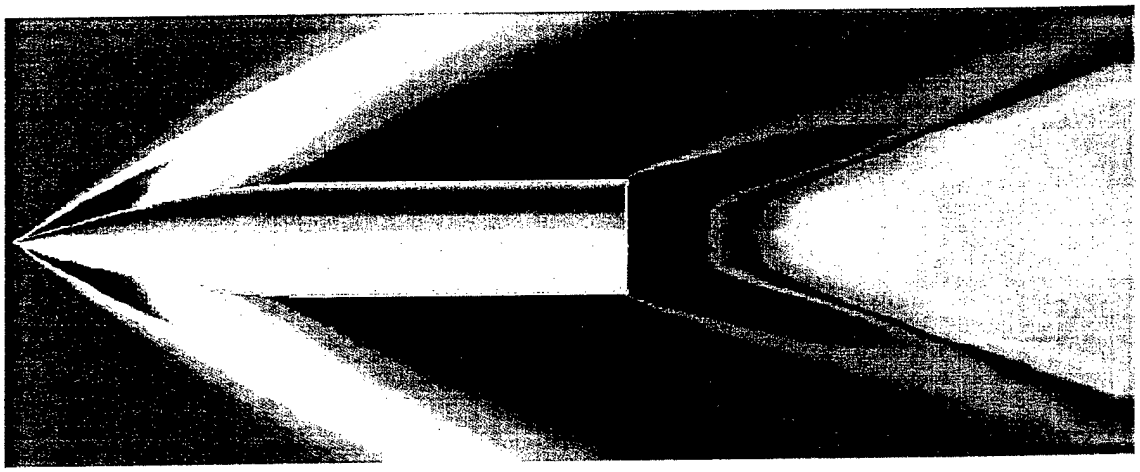

Figure 6. Pressure Contours for a Projectile Without Segments.

Computed results obtained for the projectile and the segment are presented next. The segment is placed in the wake of the projectile in the centered, offset (from center line of

symmetry), and angled (segment at angle of attack) positions. Figure 7 shows Mach contours for each of the three segment orientations. Similarly, Figure 8 shows pressure contours for each of the three segment orientations. As seen in these figures, the flow field in the wake region has changed dramatically because of the presence of the trailing segment. As expected, the flow field in the wake is still symmetrical when the segment is in the centered position. The asymmetry in

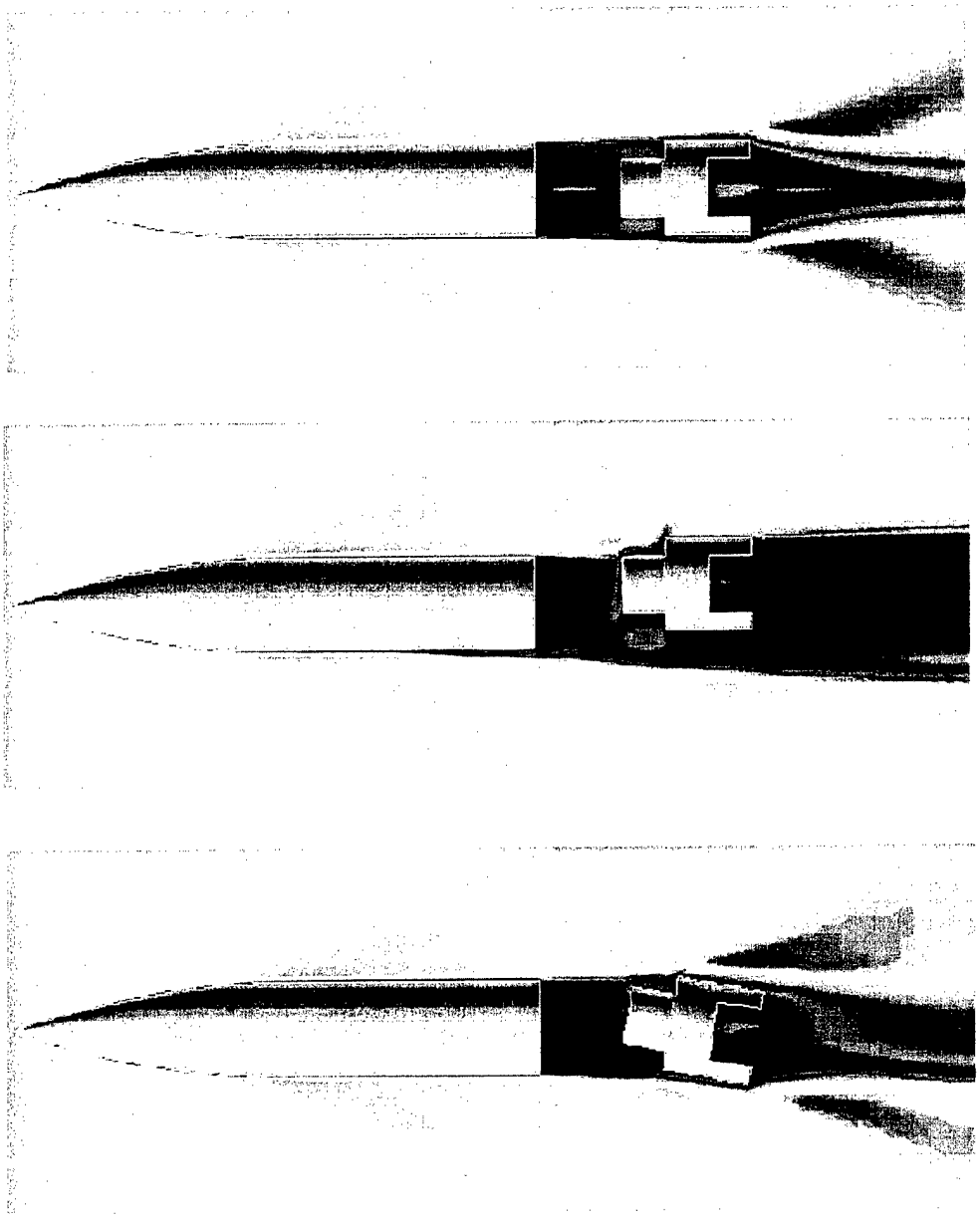

Figure 7. Mach Contours for a Segment in Three Positions: Centered, Offset, and Angled (top to bottom).

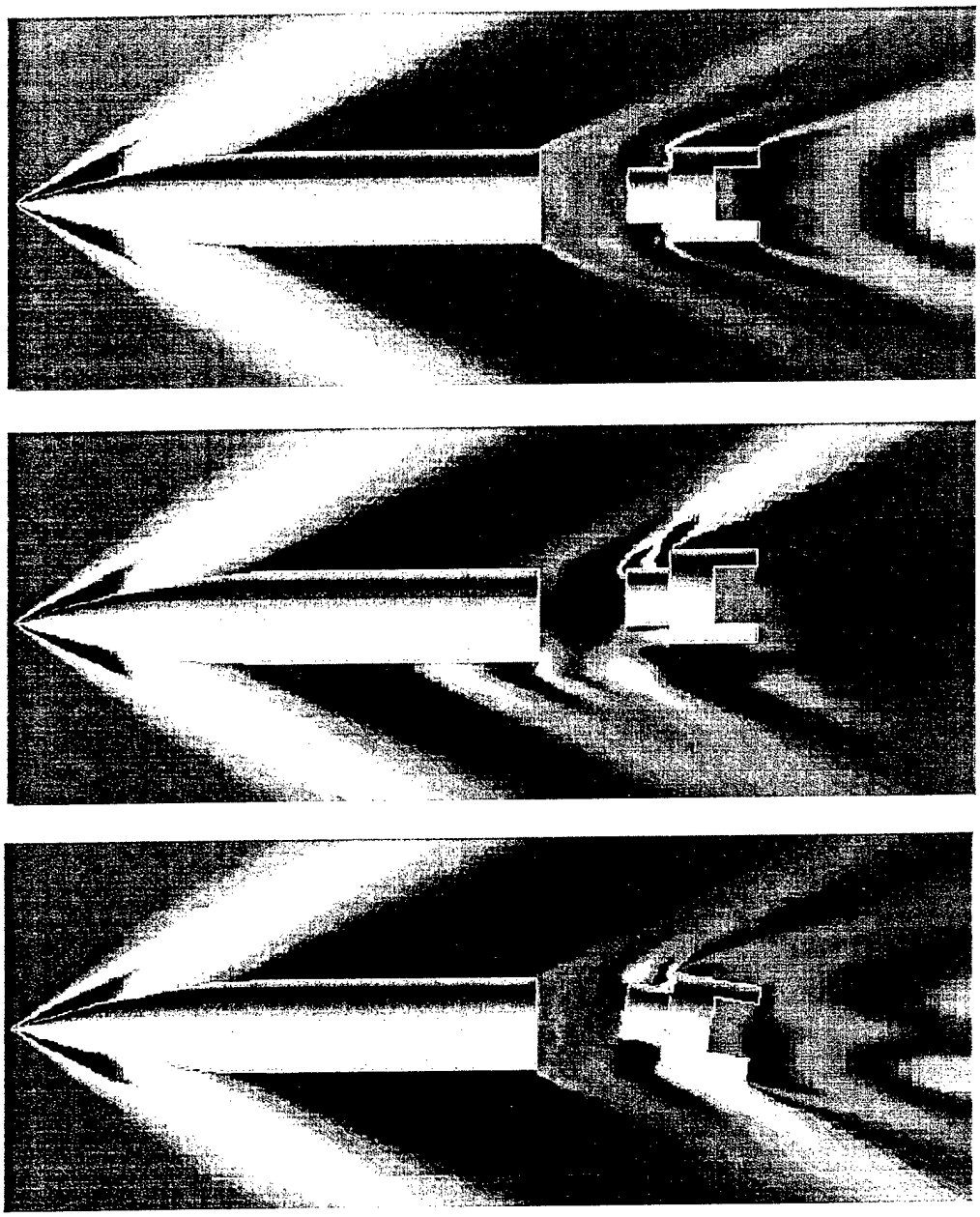

Figure 8. Pressure Contours for a Segment in Three Positions: Centered, Offset, and Angled (top to bottom).

the wake region flow can be clearly seen when the segment is in the offset and angled positions. There has been a significant increase in the width of wake region flow for the case of the segment

in the offset position (see Figure 7). In general, the pressure is higher in front of the segment and lower in the base region of the segment itself. Of the three orientations of the segment, the offset case seems to have the largest effect in the flow region between the projectile and the segment. As seen in Figure 7, the flow field in this region is quite asymmetrical. In addition, the segment in the offset position seems to have a strong effect on the flow field in the aft region of the projectile upstream from the base corner (especially in the bottom side).

Computed surface pressures on the trailing segment are quite interesting. Figure 9 shows a front view of the segments, including the peg and cylinder of the segment in each of the three positions. When the segment is centered on the line of symmetry, there is an area of high pressure along the inner and outer edges of the face of the segment behind the peg. When the segment is offset, the pressure along the face of the segment cylinder is shown to increase dramatically, especially along the upper surface of the segment peg. Finally, when the segment is in the angled position, the pressure is only slightly increased on the face of the cylinder, with a much more dramatic change along the cylinder of the segment itself. Figure 10 shows a rear view of the surface pressure in the cavity of the segment in each of the three orientations of the segment. In general, the pressure in the cavity is low for all three segment orientations, being just slightly higher when the segment is in the offset position.

Aerodynamic forces and moments have been obtained from the computed solutions. Tables 1 and 2 show some of the computed aerodynamic force and moment data for the segmented projectile system, based on the position of the segment. Both tables show the axial force (C_A), normal force (C_N), and pitching moment coefficients(C_{mp}). The presence of the segment in the wake of the projectile is expected to change these coefficients both for the projectile and the segment. Table 1 shows these coefficients for the projectile. The axial force is only slightly affected by the segment orientation; all three values are approximately 10% lower than the computed value (0.32) for the projectile-alone case. For the segment in the centered position, the flow field as explained earlier is symmetric, and therefore, the normal force and pitching moment coefficients are zero. The effect of the angled segment on the projectile force and moment is very small. The segment in the offset position has the largest effect on the force and moment coefficients of the projectile. Table 2 shows these aerodynamic coefficients for the segment itself in the three orientations. The axial force coefficient is increased somewhat when the segment is offset or angled. The offset segment has a larger axial force than that obtained for the angled segment. As for the normal force and the pitching moment coefficients, the effect is larger with the angled segment than with the offset segment.

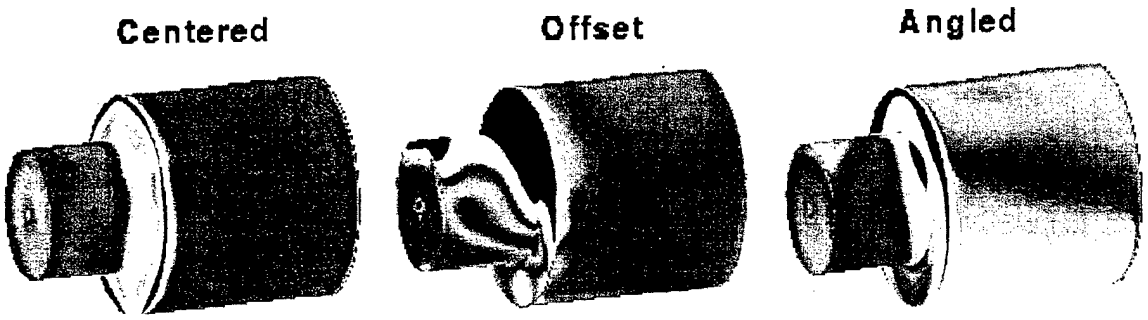

Figure 9. Surface Pressure on Segments (front view).

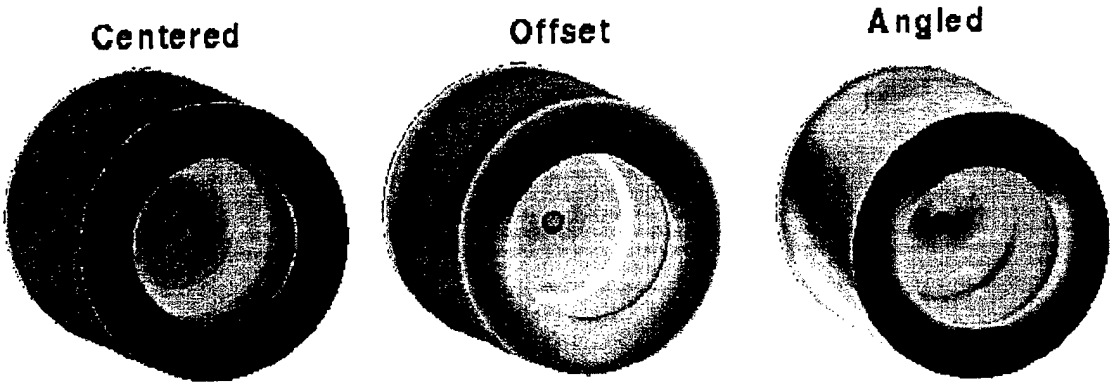

Figure 10. Surface Pressure on Segments (rear view).

Table 1

Force and Moment Data for a Projectile

Mach = 2.5 Alpha = 0.0	Segment Position		
	Centered	Offset	Angled
C_A	+0.16	+0.21	+0.19
C_N	0.00	-0.09	+0.11
C_{mp}	0.00	+0.11	-0.12

Table 2

Force and Moment Data for a Segment

Mach = 2.5	Segment Position		
Alpha = 0.0	Centered	Offset	Angled
C_A	+0.23	+0.22	+0.25
C_N	0.00	+0.04	0.00
C_{mp}	0.00	-0.16	0.00

5. CONCLUDING REMARKS

A computational study has been undertaken to compute the aerodynamics on a multi-body projectile system consisting of an ogive-cylinder projectile and a peg-shaped trailing segment. Flow field computations have been performed at Mach number $M_\infty = 2.5$ and angle of attack $\alpha = 0°$ using an unsteady, zonal F3D Navier-Stokes code and the chimera composite grid discretization technique. The computed results show the qualitative features of the wake flow field for the projectile alone, as well as with the segment in three different positions. The predicted flow field in the wake regions was seen to change dramatically in the presence of trailing segment in the wake of the projectile, especially with the segment in the offset and angled positions. Computed results also show that the segment in the offset position has a strong effect on the flow field in the aft region of the projectile upstream from the base corner and thus, on the aerodynamic force and moment coefficients of the projectile. The aerodynamic force and moment coefficients of the segment are also significantly altered, based on the orientation of the segment.

The computational analyses presented in this report show the capability of the numerical technique to compute the aerodynamic interference flow fields associated with multi-body projectile configurations. The numerical technique used here can very easily be extended to determine the aerodynamics of multiple segments flying in the wake of a parent projectile. Future efforts will therefore include numerical simulation of multi-body projectile configurations with multiple segments at (hypervelocity) flight speeds of interest.

INTENTIONALLY LEFT BLANK

REFERENCES

1. Sahu, J., and J.L. Steger. "Numerical Simulations of Transonic Flows." International Journal for Numerical Methods in Fluids, Vol. 10, No. 8, pp. 855-873, 1990.

2. Ferry, E.N., J. Sahu, and K.R. Heavey. "Navier-Stokes Computations of Sabot Discard using Chimera Scheme." Proceedings of the 16th International Symposium on Ballistics, September 1996.

3. Sahu, J., K.R. Heavey, and E.N. Ferry. "Computational Fluid Dynamics for Multiple Projectile Configurations." Proceedings of the 3rd Overset Composite Grid and Solution Technology Symposium, Los Alamos, NM, October 1996.

4. Sahu, J., and C.J. Nietubicz. "Application of Chimera Technique to Projectiles in Relative Motion," ARL-TR-590, U.S. Army Research Laboratory, Aberdeen Proving Ground, MD, October 1994.

5. Sahu, J., K.R. Heavey, and C.J. Nietubicz. "Time-Dependent Navier-Stokes Computations for Submunitions in Relative Motion." Proceedings of the 6th International Symposium on Computational Fluid Dynamics, Lake Tahoe, NV, September 1995.

6. Sahu, J., H.L. Edge, K.R. Heavey, and E.N. Ferry. "Computational Fluid Dynamics Modeling of Multi-body Missile Aerodynamic Interference," ARL-TR-1765, U.S. Army Research Laboratory, Aberdeen Proving Ground, MD, August 1998.

7. Steger, J.L., F.C. Dougherty, and J.A. Benek. "A Chimera Grid Scheme." In "Advances in Grid Generation," K N. Ghia and U. Ghia, eds., ASME FED-5, June 1983.

8. Benek, J.A., T.L. Donegan, and N.E. Suhs. "Extended Chimera Grid Embedding Scheme With Application to Viscous Flows." AIAA Paper No. 87-1126-CP, 1987.

9. Buning, P. G., I. T. Chiu, S. Obayashi, Y. M. Rizk, and J. L. Steger. "Numerical Simulation of the Integrated Space Shuttle Vehicle in Ascent." AIAA Atmospheric Flight Mechanics Conference, August 1988.

10. Pulliam, T.H., and J.L. Steger. "On Implicit Finite Difference Simulations of Three-Dimensional Flow." AIAA Journal, Vol. 18, No. 2, pp. 167–169, February 1982.

11. Steger, J.L., S.X. Ying, and L.B. Schiff. "A Partially Flux-Split Algorithm for Numerical Simulation of Compressible Inviscid and Viscous Flows." Proceedings for the Workshop on Computational Fluid Dynamics, Institute of Nonlinear Sciences, University of California, Davis, CA, 1986.

12. Suhs, N.E., and Tramel, R.W. "PEGSUS 4.0 User's Manual." AEDC-TR-8, AEDC, Tennessee, November 1991.

INTENTIONALLY LEFT BLANK

NO. OF COPIES	ORGANIZATION
2	ADMINISTRATOR DEFENSE TECHNICAL INFO CENTER ATTN DTIC OCP 8725 JOHN J KINGMAN RD STE 0944 FT BELVOIR VA 22060-6218
1	DIRECTOR US ARMY RESEARCH LABORATORY ATTN AMSRL CS AL TA REC MGMT 2800 POWDER MILL RD ADELPHI MD 20783-1197
1	DIRECTOR US ARMY RESEARCH LABORATORY ATTN AMSRL CI LL TECH LIB 2800 POWDER MILL RD ADELPHI MD 207830-1197
1	DIRECTOR US ARMY RESEARCH LABORATORY ATTN AMSRL DD J J ROCCHIO 2800 POWDER MILL RD ADELPHI MD 20783-1197
2	USAF WRIGHT AERONAUTICAL LABORATORIES ATTN AFWAL FIMG DR J SHANG MR N E SCAGGS WPAFB OH 45433-6553
1	COMMANDER NAVAL SURFACE WARFARE CNTR ATTN CODE B40 DR W YANTA DAHLGREN VA 22448-5100
1	COMMANDER NAVAL SURFACE WARFARE CNTR ATTN CODE 420 DR A WARDLAW INDIAN HEAD MD 20640-5035
4	DIRECTOR NASA LANGLEY RESEARCH CENTER ATTN TECH LIBRARY MR D M BUSHNELL DR M J HEMSCH DR J SOUTH LANGLEY STATION HAMPTON VA 23665
2	ARPA ATTN DR P KEMMEY DR JAMES RICHARDSON 3701 NORTH FAIRFAX DR ARLINGTON VA 22203-1714

NO. OF COPIES	ORGANIZATION
7	DIRECTOR NASA AMES RESEARCH CENTER ATTN MS 227 8 L SCHIFF MS 258 1 T HOLST MS 258 1 D CHAUSSEE MS 258 1 M RAI MS 258 1 P KUTLER MS 258 1 P BUNING MS 258 1 B MEAKIN MOFFETT FIELD CA 94035
1	USMA DEPT OF MECHANICS ATTN LTC ANDREW L DULL WEST POINT NY 10996
7	CDR US ARMY TACOM ARDEC ATTN AMSTA AR FSF T C NG R DEKLEINE R BOTTICELLI H HUDGINS J GRAU S KAHN W KOENIG BLDG 382 PICATINNY ARSENAL NJ 07806-5000
1	CDR US ARMY TACOM ATTN AMSTA AR CCH B P VALENTI BLDG 65-S PICATINNY ARSENAL NJ 07806-5001
1	COMMANDER US ARMY ARDEC ATTN SFAE FAS SD MIKE DEVINE PICATINNY ARSENAL NJ 07806-5001
1	COMMANDER US NAVAL SURFACE WEAPONS CTR ATTN DR F MOORE DAHLGREN VA 22448
2	UNIV OF CALIFORNIA DAVIS DEPT OF MECHANICAL ENG ATTN PROF H A DWYER PROF M HAFEZ DAVIS CA 95616
1	AEROJET ELECTRONICS PLANT ATTN DANIEL W PILLASCH PO BOX 296 B170 DEPT 5311 1100 WEST HOLLYVALE ST AZUSA CA 91702

NO. OF COPIES	ORGANIZATION
3	AIR FORCE ARMAMENT LAB ATTN AFATL/FXA S C KORN B SIMPSON D BELK EGLIN AFB FL 32542-5434
1	MASSACHUSETTS INST OF TECH ATTN TECH LIBRARY 77 MASSACHUSETTS AVE CAMBRIDGE MA 02139
1	GRUMANN AEROSPACE CORP AEROPHYSICS RESEARCH DEPT ATTN DR R E MELNIK BETHPAGE NY 11714
2	MICRO CRAFT INC ATTN DR JOHN BENEK NORMAN SUHS 207 BIG SPRINGS AVE TULLAHOMA TN 37388-0370
1	LOS ALAMOS NATIONAL LAB ATTN BILL HOGAN MS G770 LOS ALAMOS NM 87545
3	DIR SANDIA NATL LABORATORIES ATTN DIV 1554 DR W OBERKAMPF DIV 1554 DR F BLOTTNER DIV 1636 DR W WOLFE ALBUQUERQUE NM 87185
1	NAVAL AIR WARFARE CENTER ATTN D FINDLAY MS 3 BLDG 2187 PATUXENT RIVER MD 20670
1	METACOMP TECHNOLOGIES INC ATTN S R CHAKRAVARTHY 650 HAMPSHIRE ROAD SUITE 200 WESTLAKE VILLAGE CA 91361-2510
2	ROCKWELL SCIENCE CENTER ATTN S V RAMAKRISHNAN V V SHANKAR 1049 CAMINO DOS RIOS THOUSAND OAKS CA 91360
1	ADVANCED TECHNOLOGY CTR ARVIN/CALSPAN AERODYNAMICS RESEARCH DEPT ATTN DR M S HOLDEN PO BOX 400 BUFFALO NY 14225

NO. OF COPIES	ORGANIZATION
1	PENNSYLVANIA STATE UNIV DEPT OF AEROSPACE ENGG ATTN DR G S DULIKRAVICH UNIVERSITY PARK PA 16802
1	UNIV OF ILLINOIS AT URBANA CHAMPAIGN DEPT OF MECHANICAL AND INDUSTRIAL ENGINEERING ATTN DR J C DUTTON URBANA IL 61801
1	UNIVERSITY OF MARYLAND DEPT OF AEROSPACE ENGG ATTN DR J D ANDERSON JR COLLEGE PARK MD 20742
1	UNIVERSITY OF NOTRE DAME DEPT OF AERONAUTICAL AND MECHANICAL ENGINEERING ATTN PROF T J MUELLER NOTRE DAME IN 46556
1	UNIVERSITY OF TEXAS DEPT OF AEROSPACE ENG MECHANICS ATTN DR D S DOLLING AUSTIN TX 78712-1055
1	UNIVERSITY OF DELAWARE DEPT OF MECHANICAL ENG ATTN DR JOHN MEAKIN NEWARK DE 19716
4	COMMANDER USAAMCOM ATTN AMSAM RD SS AT ERIC KREEGER GEORGE LANDINGHAM CLARK D MIKKELSON ED VAUGHN REDSTONE ARSENAL AL 35898-5252
1	COMMANDER US ARMY TACOM ARDEC ATTN AMCPM DS MO P J BURKE BLDG 162S PICATINNY ARSENAL NJ 07806-5000
	ABERDEEN PROVING GROUND
2	DIRECTOR US ARMY RESEARCH LABORATORY ATTN AMSRL CI LP (TECH LIB) BLDG 305 APG AA

NO. OF COPIES	ORGANIZATION
2	DIR USARL ATTN AMSRL WM I MAY L JOHNSON BLDG 4600
2	DIR USARL ATTN AMSRL WM B A W HORST JR W CIPEIELLA BLDG 4600
1	DIR USARL ATTN AMSRL WM B E M SCHMIDT BLDG 4600
3	DIR USARL ATTN AMSRL WM BA W D'AMICO F BRANDON T BROWN BLDG 4600
1	DIR USARL ATTN AMSRL WM BD B FORCH BLDG 4600
3	DIR USARL ATTN AMSRL WM BE G WREN M NUSCA J DESPIRITO BLDG 390
1	DIR USARL ATTN AMSRL WM BF J LACETERA BLDG 120
20	DIR USARL ATTN AMSRL WM BC P PLOSTINS D LYON M BUNDY G COOPER J GARNER B GUIDOS K HEAVEY H EDGE V OSKAY A MIKHAIL J SAHU K SOENCKSEN D WEBB P WEINACHT S WILKERSON A ZIELINSKI BLDG 390
1	DIR USARL ATTN AMSRL CI C NIETUBICZ BLDG 394
1	DIR USARL ATTN AMSRL DI H W STUREK BLDG 328

NO. OF COPIES	ORGANIZATION
3	CDR US ARMY ARDEC FIRING TABLES BRANCH ATTN R LIESKE R EITMILLER F MIRABELLE BLDG 120
	ABSTRACT ONLY
1	DIRECTOR US ARMY RESEARCH LABORATORY ATTN AMSRL CS AL TP TECH PUB BR 2800 POWDER MILL RD ADELPHI MD 20783-1197

INTENTIONALLY LEFT BLANK

REPORT DOCUMENTATION PAGE

Form Approved
OMB No. 0704-0188

1. AGENCY USE ONLY *(Leave blank)*	2. REPORT DATE	3. REPORT TYPE AND DATES COVERED
	June 1999	Final

4. TITLE AND SUBTITLE

Computational Modeling of a Segmented Projectile

5. FUNDING NUMBERS

PR: 1L162618AH80

6. AUTHOR(S)

Sahu, J.; Heavey, K.R. (both of ARL)

7. PERFORMING ORGANIZATION NAME(S) AND ADDRESS(ES)

U.S. Army Research Laboratory
Weapons & Materials Research Directorate
Aberdeen Proving Ground, MD 21010-5066

8. PERFORMING ORGANIZATION REPORT NUMBER

9. SPONSORING/MONITORING AGENCY NAME(S) AND ADDRESS(ES)

U.S. Army Research Laboratory
Weapons & Materials Research Directorate
Aberdeen Proving Ground, MD 21010-5066

10. SPONSORING/MONITORING AGENCY REPORT NUMBER

ARL-TR-1988

11. SUPPLEMENTARY NOTES

12a. DISTRIBUTION/AVAILABILITY STATEMENT

Approved for public release; distribution is unlimited.

12b. DISTRIBUTION CODE

13. ABSTRACT *(Maximum 200 words)*

This report describes the application of the chimera numerical technique to a multi-body segmented projectile configuration system of interest to the U.S. Army. Computations were performed at a supersonic speed on this configuration which consists of an ogive-cylinder projectile with a peg-shaped trailing segment. The computed results show the qualitative features of the wake flow field for the projectile with the segment in three different positions: centered, offset, and angled. The segment in the offset position has a strong effect on the flow field in the aft region of the projectile, thus affecting the aerodyamic coeffiecients of the projectile. The force and moment coefficients of the segment are also significantly affected by the orientation of the segment.

14. SUBJECT TERMS

aerodynamic coefficients; computational fluid dynamics; supersonic flow; Chimera technique; mult-ibody; wake flow field

15. NUMBER OF PAGES
30

16. PRICE CODE

17. SECURITY CLASSIFICATION OF REPORT	18. SECURITY CLASSIFICATION OF THIS PAGE	19. SECURITY CLASSIFICATION OF ABSTRACT	20. LIMITATION OF ABSTRACT
Unclassified	Unclassified	Unclassified	